IEEE Robotics and Automation Letters (RAL) paper presented at
2024 IEEE/RSJ International Conference on Intelligent Robots and Systems (IROS)
October 14-18, 2024. Abu Dhabi, UAE

ALBERO: Agile Landing on Branches for Environmental Robotics Operations

Liming Zheng and Salua Hamaza

***Abstract*—Drones have been increasingly used in various domains, including ecological monitoring in forests. However, the endurance and noise of drones have limited their deployment to short flight missions above canopies. To address these limitations, we introduce ALBERO: a framework comprising a mechanical solution and an optimal planner to realise agile quadrotor perching on tree branches of steep incline. The gripper features an ultra-fast active mechanism inspired by birds' claws that enables quadrotors to perch swiftly on randomly-oriented tree branches. By perching, the drone can preserve energy for extended periods of time, while silently gathering forest data in the canopy. The intrinsic properties of the gripper allow for extra flexibility in size, surface roughness and shape imperfections of natural perches, such as those found in the wild. The gripper also has good scalability properties and can be easily matched to different drones' sizes and weights. The biggest advantage of this novel design lays in its ability to close reactively and ultra-fast (67 *ms* on the large gripper, 42 *ms* on the small gripper), enabling the quadrotor to perform agile perching manoeuvres from different angles and at different approach speeds. ALBERO's software module comprises of a trajectory planning algorithm adapted for branch perching, ensuring that the drone can perch on inclined cylindrical targets from any starting location in the proximity of the branch. These requirements translate in stringent positioning and orientation accuracy, but they enable the drone to land dynamically from a variety of positions within the forest.**

***Index Terms*—Agile Perching, Agile Motion Planning, UAVs Applications, Gripper Design, Environmental Monitoring.**

I. Introduction

THE ongoing degradation of forests and the associated decline in biodiversity have prompted increased efforts to devise protective strategies for these ecosystems [1]–[3]. Historically, conservation methodologies relied heavily on experienced human resources for deploying sensors or establishing observation towers [4]. However, there's been a progressive shift towards harnessing robotic technologies to facilitate these tasks [5], offering enhanced efficiency, scalability, and most notably, a reduced environmental footprint within pristine forest habitats. Drones capable of navigating a vast three-dimensional forest space are particularly apt for tasks such as placing sensors [6]–[8] at different heights of the forest strata, or gathering biological specimens [9]. Yet, drones' operational duration (battery life) and noise emissions remain prominent hurdles to their extensive deployment within forest settings [10]: the limited endurance directly impacts mission duration, while the generated noise can interfere with the natural activities of forest inhabitants [11].

Fig. 1: Agile quadrotor perching on tree branches of steep incline during XPRIZE Rainforest semifinals, Singapore 2023.

To address the dual challenges of endurance and noise, a biomimetic approach termed "perching" is investigated. Perching denotes birds' ability to land on and latch on tree branches. Perching drones can exploit this state to extend flight time by preserving energy: by shutting off their propellers while perched, drones can remain stationary and silent, efficiently harnessing environmental, acoustic, and visual forest data. Once the data collection is complete, the drone can relaunch, transitioning to another perching location for prolonged and sustained data acquisition.

The growth direction of branches within forests is influenced by a myriad of factors, including species, age, light exposure, gravity, wind direction, and humidity, etc [12]–[14]. To maximize light absorption, most trees tend to grow their branches outward and upward, resulting in the majority of branches being inclined rather than horizontal. Consequently, if drones are only equipped to land on horizontal branches, they may expend considerable flight time searching for such branches. This increased search time can significantly deplete the drone's endurance, and in some areas, might even prevent successful perching altogether. Various mechanisms have been devised to enable aerial perching with drones [15]–[21]. Examples include an optimized perching gripper [15], drone arms designed in a bistable manner [16], [17], and claw designs specialized for flapping-wing drones [22]. For drones aiming to perch on horizontal branches, the requirements for gripper closure time

Manuscript received: August 15, 2023; Revised: November 4, 2023; Accepted: December 14, 2023.

The authors are with the BioMorphic Intelligence Lab, Department of Control & Operations, Faculty of Aerospace Engineering, TU Delft, The Netherlands. E-mail correspondence: l.zheng-1@tudelft.nl

and force aren't particularly stringent, thanks to the fact that the drone can hover in proximity of the target for as long as needed for the gripper to secure the grasp. The same does not apply for inclined perches, where a quadrotor cannot maintain any given pose for longer than a few milliseconds. This is the reason why all existing methods leveraging a mechanical solution primarily focused on horizontal targets.

However, perching on inclined branches presents new challenges since the gripping mechanism must rapidly secure the hold, given that quadrotors cannot maintain an inclined orientation whilst airborne. To this end, other studies have focused on agile motion planning methods for landing on flat surfaces and overhangs [10], [23]–[26]. For instance, the work of [10] employed electroadhesive materials to perch on overhangs made of plywood, glass, and leaves. Another study [23] used a magnet attached at the drone's base to perch on slanted metal surfaces, leveraging MINCO (minimum control) trajectory planning [27]. Additionally, [24] utilized Velcro to perch on inclined surfaces. While these mechanisms are subject to strict surface conditions, rendering them unsuitable for forests and presenting relaunch challenges, the agility they exhibit in dynamic perching via trajectory planning is undeniably exceptional.

This work proposes an approach that integrates ultra-fast mechanical grasping with trajectory planning for robust quadrotor perching on randomly-oriented tree branches. The focus on inclined branches is of high relevance for real-world deployment of drones in forest missions, extending drones' flexibility for field operations. We introduce a framework, named ALBERO, that utilizes bistable materials for energy storage and active grasping, complemented with trajectory planning for agile perching. ALBERO's key features include:

- ultra-fast mechanical grasping upon contact (large gripper close time is $0.067s$, small gripper is only $0.042s$);
- motion planning for agile landing on branches of steep incline;
- scalability: the gripper is modular and can be easily integrated on off-the-shelf quadrotors of different sizes;
- energy-efficient, requiring energy only in the instant of perching, with no energy consumption during flight to hold a specific configuration;
- extremely high power-to-weight ratio, representing less of a burden on battery life and mission time;
- higher technology readiness level (TRL): the above features enable aerial perching in more realistic scenarios, advancing drones' readiness in field operations.

ALBERO's gripper was further validated during XPRIZE Rainforest semifinals in Singapore, July 2023, during manual flight tests in the tropical rainforest, see Figs. 1 and 6 (D-F).

II. Gripper Design

The design inspiration for ALBERO is derived from the slap bracelet, a bistable material recognized for its rapid closure, cost-effectiveness, and high force-to-weight ratio. We use servomotors to drive the active opening and closing of the gripper. In this context, passive closing would necessitate the drone to apply a significant force, in bouncing on the perch upon contact, leading to failure. One approach to counter this is by designing a new drone's body made of soft materials and capable of shock absorption via means of an air-pump [28]. To address this issue in our study, we employ two distinct servomotors to control the opening and closing of the gripper independently. , while still reaching ultra-fast performance. Moreover, ALBERO offer scalability to drones of different sizes by modifying the quantity and length of spring bands stacked on each other.

A. Working Principle

The gripper features a symmetrical structure along its longitudinal plane, integrating the energy storage attributes of deformable spring steel with servo actuators. Spring steel bands offer two stable states: straight and curled. For quick grasping, we use pre-formed bi-stable spring steel that respond immediately to orthogonal contact, delivering high energy upon closure. To re-open, we devise a system with a pulley can gears that uncurls the spring steel open. Previous methods that used similar materials relied on pressured air to transition between closed and open state [28]. In their work, the closing phase was initiated by drone drop landing on the perching target from a hover position, reaching a drop speed of approximately 2.4 m/s. This way, a high enough force would set the gripper to close passively. While drop landing on the target was well suited for the soft-bodied drone presented by the authors, this method cannot be effectively integrated on standard rigid-bodied drones because of the bouncing motion that the drop causes.

To seamlessly integrate the gripper with traditional rigid-bodied drones, we have designed the gripper to be actively controlled. Our design ensures a robust curled state and a permanent semi-stable state. This semi-stable configuration biases the spring steel towards closure, even in the opened position. A trigger mechanism (see Fig. 2A) is devised to enforce this partially stable state. By disengaging the trigger, the gripper promptly closes from the semi-stable state. A rigid bar pushing on the middle section of the spring bands (see Fig. 2E) exerts a continuous force that maintains the semi-stable state, favouring the curling motion. In addition, to re-open the gripper and flatten the spring bands, we devise a support structure (see Fig. 2A) with a tip (see Fig.2F) featuring two protrusions, S_1 and S_2. These aid a smooth opening of the tip of the gripper under the traction force F_o. In the results section, we demonstrate the opening performance of the gripper at various positions and heights of the support.

We use two types of servos in our gripper system. The first is a 360° servo for tightening and loosening the fishing line attached to the spring steel. The second is a 180° servo that controls the trigger's state. Here's how the gripper works: the 360° servo tightens the line when the spring steel is straight. Then, the 180° servo positions the trigger for stability. Reversing the 360° servo relaxes the line. As the drone approaches the branch, the 180° servo triggers the gripper to grasp the branch. At take-off, the propellers rotate, the 360° servo tightens the line to open the gripper, and the drone lifts off. The 180° servo resets the trigger's position, and the gripper is ready for the next perching operation.

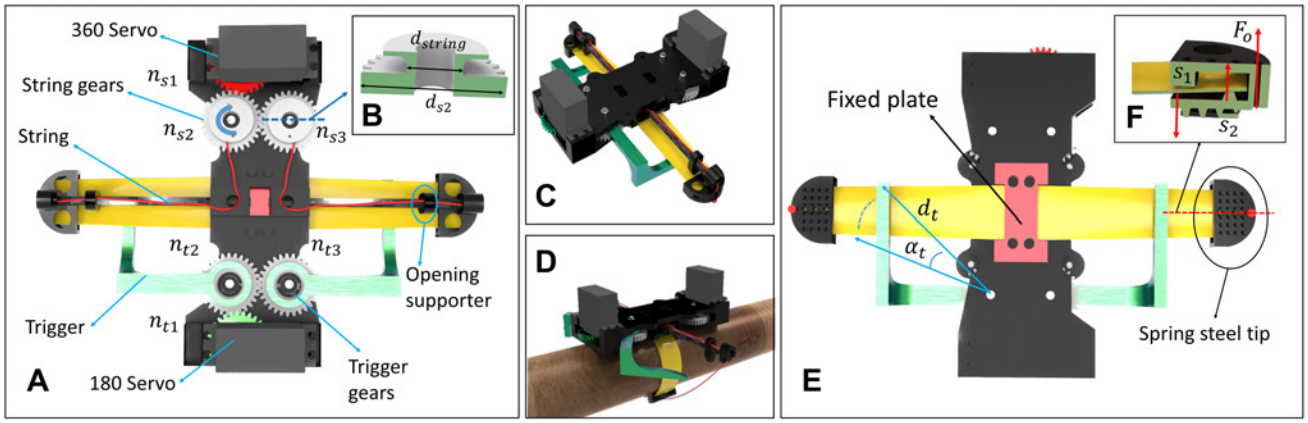

Fig. 2: ALBERO's schematic diagram: A) Gripper cutaway showing the position of the coiling gears and path of the string, B) Cross-sectional view of string gear along the blue dashed line, C) Opening of the gripper, D) Perching onto a tree branch, E) Gripper's bottom view and F) trigger mechanism stabilising the finger along the red dashed line.

B. Analysis

We use symmetrical gears to allow a single servo to drive both fingers simultaneously, achieving a balance between grasping speed and torque with an optimized gear ratio. This setup also lightens the torque demand on the servo. As shown in Fig. 2, the 360° servo gear has n_{s1} teeth and a diameter of d_{s1}. The driven gear has n_{s2} teeth and a diameter of d_{s2}. The string's unwinding diameter is d_{string}. In the top view, the positive rotation of gear n_{s2} is clockwise. The symmetrical gear on the opposite end, ensuring identical finger movement, has n_{s3} teeth. Thus, $n_{s2} = n_{s3}$. The required torque M_c for the 360° servo is calculated as follows:

$$M_c = \frac{F_s d_{string} d_{s1}}{d_{s2}}. \tag{1}$$

The maximum rotation speed of a general 360° servo is fixed and assumed to be $\omega_{c\max}$. Thus, the string's movement speed v_{string} can be calculated as follows:

$$v_{string} = \frac{d_{s1}\omega_{c\max} d_{string}}{2d_{s2}}. \tag{2}$$

The formula shows that the torque required for the 360° servo increases with larger values of d_{s1} and d_{string}, and smaller values of d_{s2}. A larger torque results in a faster movement of the string. The distance between the 180° servo trigger and the rotation axis is denoted by $d_{trigger}$, and when the servo rotates by an angle of α, the fingers are released. This angle can be used to calculate the time required for the trigger to move, denoted by $t_{trigger}$:

$$t_{trigger} = \frac{\alpha d_{t2}}{\omega_{n\max} d_{t1}}. \tag{3}$$

The maximum rotation speed of the 180° servo is denoted by $\omega_{n\max}$. It can be inferred from the equation that the size of α is negatively correlated with the size of $d_{trigger}$. Hence, increasing $d_{trigger}$ will reduce the required time. Conversely, the larger the value of d_{t2}, the larger the value of α, and the smaller the value of d_{t1}, the longer the required time. This is not desirable for perching, as it could compromise the stability and accuracy of the gripper's movement. Therefore, it is important to carefully choose the dimensions of the trigger and the associated components.

Fig. 3: Gripper mechanism for agile quadrotor perching.

C. Manufacturing

Our gripper design offers significant scalability advantages. The number of spring steel layers can be customised to fit drones of different sizes, and the driving force required to grasp robustly can be achieved by selecting an appropriate servo. To determine the necessary grasping force, we conducted experiments that are presented in the Results section. The gripper components are 3D printed using PLA and PAHT-CF. The ALBERO gripper features a number of identical spring steel layers stacked onto each other, each with a thickness of 0.5 *mm*. In the closed state, the spring bands lay fully flat onto the target, while they present a slight curve in the open state. To demonstrate the scalability of our gripper, we design two variants: a larger model measuring 200 *mm* in length, and a smaller version of 110 *mm*, allowing for seamless integration with drones of corresponding sizes. To connect multiple spring steel layers, a stiff string binds the layers together and ties them on two holes at both ends of the gripper. To better cope with different types of bark and trees upon grasping, the thickness and reliability of the gripper were further improved by adding a neoprene adhesive film and Dycem Non-slip foil, highly frictional material. These improved the ergonomics of the gripper for various types of wood and surface's roughness.

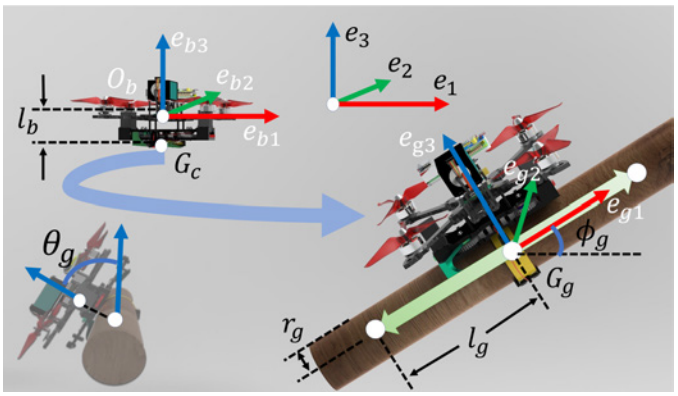

Fig. 4: Modeling overview and symbols definition.

III. Agile Perching on Trees

To perch quadrotors dynamically on inclined cylinders, we want to control the pose of the drone at all stages of the maneuvre, especially in the final state upon contact. This represents a trajectory planning problem that has been addressed for free-flying quadrotors using various methods. One approach involves treating it as a quadratic programming (QP) problem [26] and using linear approximations, but this method cannot adjust the flight time. [24] addresses the active visual perching (AVP) control for autonomous micro aerial vehicles to perch on inclined surfaces, leveraging the Karush–Kuhn–Tucker (KKT) conditions for real-time trajectory planning, optimizing target visibility, and demonstrating improved accuracy and success rates compared to one-shot planning, even under significant computational constraints. Other methods such as nonlinear programming (NLP) have also been proposed [29]. A recent study [23] used the Minimum Control (MINCO) [27] trajectory optimization-based framework and compared it with NLP. The results demonstrated that MINCO used fewer computational resources than NLP. Based on these efforts, we build upon the MINCO algorithm and further develop it to solve the problem of agile quadrotor perching on tree branches.

A. Modeling

We employ the simplified dynamics proposed by [30] for a quadrotor. The configuration of the quadrotor is defined by its translation $p \in \mathbb{R}^3$ and rotation $R \in \mathbb{R}^{3\times3}$. The translational motion is affected by the gravitational acceleration g and the thrust f, while the rotational motion is influenced by the body rate $\omega \in \mathbb{R}^3$. The simplified model can be expressed as follows:

$$\begin{cases} \tau = fR\mathbf{e}_3/m, \\ \ddot{p} = \tau - g\mathbf{e}_3, \\ \dot{R} = R\hat{\omega}, \end{cases} \tag{4}$$

Let τ represent the total thrust, $\mathbf{e}_i$ denote the i-th column of the identity matrix $\mathbf{I}_3$, and $\hat{\cdot}$ signify the skew-symmetric matrix corresponding to the vector cross product. The shapes of tree branches in nature are diverse, but a small portion of them can be approximated by a cylindrical shape with varying cross-sectional areas. In this study, we assume that for branches within the specific range $(-l_g, l_g)$, the mean radius is represented by r_g, and the central point of the branch is denoted as G_g. Here, $\mathbf{e}_{gi}$ represents the i-th column of the branch body frame. $\mathbf{e}_{g1}$ aligns with the branch's axis, while $\mathbf{e}_{g3}$ lies within the plane defined by $\mathbf{e}_{g1}$ and the vertical direction. The corresponding coordinate system is designated as $\mathscr{O}_g$. The surface position of a suitable landing spot on the branch can be represented as $\mathbf{B}(t)$, as follows:

$$\mathbf{B}(t) = \left\{ x = R_g(t)\mathbf{D}r_g u + c_g(t) \;\middle|\; \|u\| = 1, u \in \mathbb{R}^2 \right\} \tag{5}$$

where $\mathbf{D} = (\mathbf{e}_2, \mathbf{e}_3) \in \mathbb{R}^{3\times2}$, and the average central axis position coordinates of the branch are denoted as $c_g(t) = G_g(t) + \lambda e_{g1}, \lambda \in (-l_g, l_g)$.

B. Motion Planning

Once the specific location of the tree branch is known, we aim to generate a smooth dynamic perching trajectory $p(t)$ that has a final velocity of a small magnitude, perpendicular to the branch. This is an important requirement as it ensures that the drone does not slip after perching, based on the gripper's grasping force performance (see Results section). To satisfy these requirements, we propose the following optimization-based perching method:

$$\min_{p(t),T} \mathscr{J} = \int_0^T \|p^{(s)}(t)\|^2 dt + \rho T, \tag{6a}$$

$$s.t. \quad T > 0, \tag{6b}$$

$$p^{[s-1]}(0) = \mathbf{p}_0 \tag{6c}$$

$$p(T) - l_b \mathbf{z}_b(t) = \mathbf{B}(T) \tag{6d}$$

$$\theta_g(T) \le \theta_{g,\max} \tag{6e}$$

$$p(T)^{(1)} = [0,0,0] \quad \text{(in the ideal case)} \tag{6f}$$

$$\|p^{(1)}(t)\| \le v_{\max} \tag{6g}$$

$$\|\omega(t)\| \le \omega_{\max} \tag{6h}$$

$$\tau_{\min} \le \|\tau(t)\| \le \tau_{\max} \tag{6i}$$

$$\mathbf{e}_3^T p(t) \ge z_{\min} \tag{6j}$$

Where Eq. (6a) trades off the smoothness and aggressiveness; (6c) is the boundary conditions of initial state; (6d) is the terminal position on the surface of the branch; the distance l_b represents the separation between the center of gravity and the gripper's surface; (6e) indicates that the angle θ_g at the final state should be smaller than the maximum angle at which the drone can perch safely without slipping. This maximum angle is calculated using Eq. (7), where $M_{\max}$ represents the gripper's maximum torque for the target branch, see Results section. This requirement ensures that the drone's propellers face upwards when it successfully perches on the branch.

$$(l_b + r_g) mg \cos\phi_g \sin\theta_g \le M_{\max} \tag{7}$$

In the ideal case, the terminal velocity should be $[0,0,0]$. (6g)-(6j) are respectively the constraints on velocity, angular velocity, thrust, and flight altitude.

As in [23], we also use MINCO with $s = 4$ and N-piece for

minimum snap and enough freedom of optimization. Then the gradients $\partial \mathscr{J}_0/\partial c_i$ and $\partial \mathscr{J}_0/\partial T_i$ can be evaluated as:

$$\frac{\partial \mathscr{J}_0}{\partial c_i} = 2\left(\int_0^{T_i} \beta^{(3)}(t)\beta^{(3)}(t)^T dt\right) c_i \tag{8a}$$

$$\frac{\partial \mathscr{J}_0}{\partial T_i} = c_i^T \beta^{(3)}(T_i)\beta^{(3)}(T_i)^T c_i + \rho \tag{8b}$$

Where $\beta(t) = (1, t, ..., t^N)^T$ is the natural basis.

IV. Results

We conducted experiments to validate the ALBERO framework. Using a high-frame-rate camera, we recorded the grippers' actions to measure its speed. The gripper design was assessed using the Zwich universal tensile machine, see in Fig.5A, with a 100N loadcell measuring force. Characterization experiments were conducted to gauge payload capacity, perching torque, opening force, and trigger rotation force. Based on these results, we made grippers for UAVs weighing 950g and 148g, highlighting our design's scalability. Finally, indoor and outdoor tests demonstrate ALBERO's ability to perch on branches of different inclines.

A. Ultra-fast Grasping

High-speed camera recordings (240 fps) of ALBERO's closure mechanism show two distinct phases. Initially, the trigger, powered by a servomotor (see Fig. 2A), disengages from the spring steel, requiring 21 *ms* for both gripper sizes. Subsequently, the larger gripper latches onto an object within 46 *ms*, culminating in total of 67 *ms* from commanded input (see Fig.6G-I). The smaller gripper achieves the same grasp in 21 *ms*, and 42 *ms* for the entire process (see Fig.6J-L).

B. Gripper Characterisation Experiments

To assess the gripper's grasp, we performed a max payload test. We secured branches of various sizes on a Zwick universal tensile machine's upper surface, and affixed the gripper with varying metal sheet quantities on the moving plate below. Gradually lowering the platform, we recorded max force as the gripper released the branch. We tested 1 to 10 spring steel layers, with 6 trials per quantity, then averaged results. Fig. 5B depicts a linear link between grasping force and steel layers. Linear regression analysis yielded the equation:

$$F_{grasp} = 4.05 n_{steel} - 0.82 \tag{9}$$

For each added spring steel band, the lifting capacity increases by 4.05N. Our experimental tree branches presented various surface roughness and were not perfectly cylindrical, prompting multiple tests for accuracy. A typical 5-inch quadrotor can carry about 1kg. Considering a 2g overload during perching, a gripping force of 20N is essential. A gripper with six spring steel layers provides roughly 22N of force. We tested this on four branch sizes found in the forest, ranging from 54 *mm* to 103 *mm*. Fig. 5C shows a negative relationship between gripping force and branch size, with the weight capacity rising as the branch size decreases. Notably, with smaller branches, the metal bands at both ends may overlap onto each other, resulting in an even better grasp.

C. Grasping Friction on Tree Bark

To enhance the gripper's friction, we applied Dycem Non-slip material on its surface. To ensure the maximum permissible inclination angle θ_g for the drone to safely perch, we positioned the gripper horizontally on a tree branch, specifically when $\theta_g = 90^o$, and gradually increased the pulling force at a distance of 40 *mm* from the gripper surface to assess the force required to induce slipping. The results reveal the maximum degree of slippage the drone may encounter on various tree branches, see in Fig. 5F. To ensure a secure landing on a tree branch, we set the $\theta_{g,max}$ below 40^o.

D. Trigger Force

The selection of the trigger servo is primarily based on the torque needed to activate the trigger, while the force required to open the trigger is determined by the friction between the trigger and its contacting components. To enhance the grip's friction with the branches, we employed Dycem Non-slip material, significantly boosting the frictional force. However, this material hinders the trigger's opening, as it necessitates a higher torque to actuate. Experimental findings demonstrated that when utilizing a gripper with six metal sheets, a force of 22.37N was needed to activate the trigger. Nevertheless, by applying paper tape to the surface, the required force reduced to only 5.47N, as illustrated in Fig. 5E.

E. Gripper Re-opening Characterisation

In our experiment, we assessed the force required to open a single "finger" of the symmetrically designed gripper using a six-band metal configuration. The results in Fig.5I reveal three stages of the opening force. We marked points A, B, and C on the finger (Fig. 5G), representing the fixed base, the position making contact with the opening support, and the tip of the finger, respectively. Initially, when A-C are curled a steady force F_{o1} of about 6.0N is noted. When point B contacts the support, the force increases to a peak F_{o2}, then drops, indicating near full opening of the A-B portion. The B-C segment opens last, demanding the highest force, culminating in a latch placement to maintain stability.

We also conducted experiments to test the force required to open the finger at different heights h_s and positions l_s of the opening support. The experimental results of Fig. 5H demonstrate that when the height is less than 20mm, the force F_{o1} remains consistent as h_s gradually increases, while F_{o2} gradually increases, and F_{o3} remains nearly constant. However, when the height h_s increases to 25mm, F_{o2} also increases to 16N, and the third stage concludes quickly after the second stage, leading to a single peak. Regarding the supports at different positions l_s, the force required to open A-B decreases, indicated by a decrease in F_{o2}, when the support gets closer to point A, see Fig.5I. However, F_{o3} remains at a consistent level, irrespective of the support's position.

F. Scalability

To demonstrate the scalability of our gripper design, we developed two different sizes of grippers for drones weighing

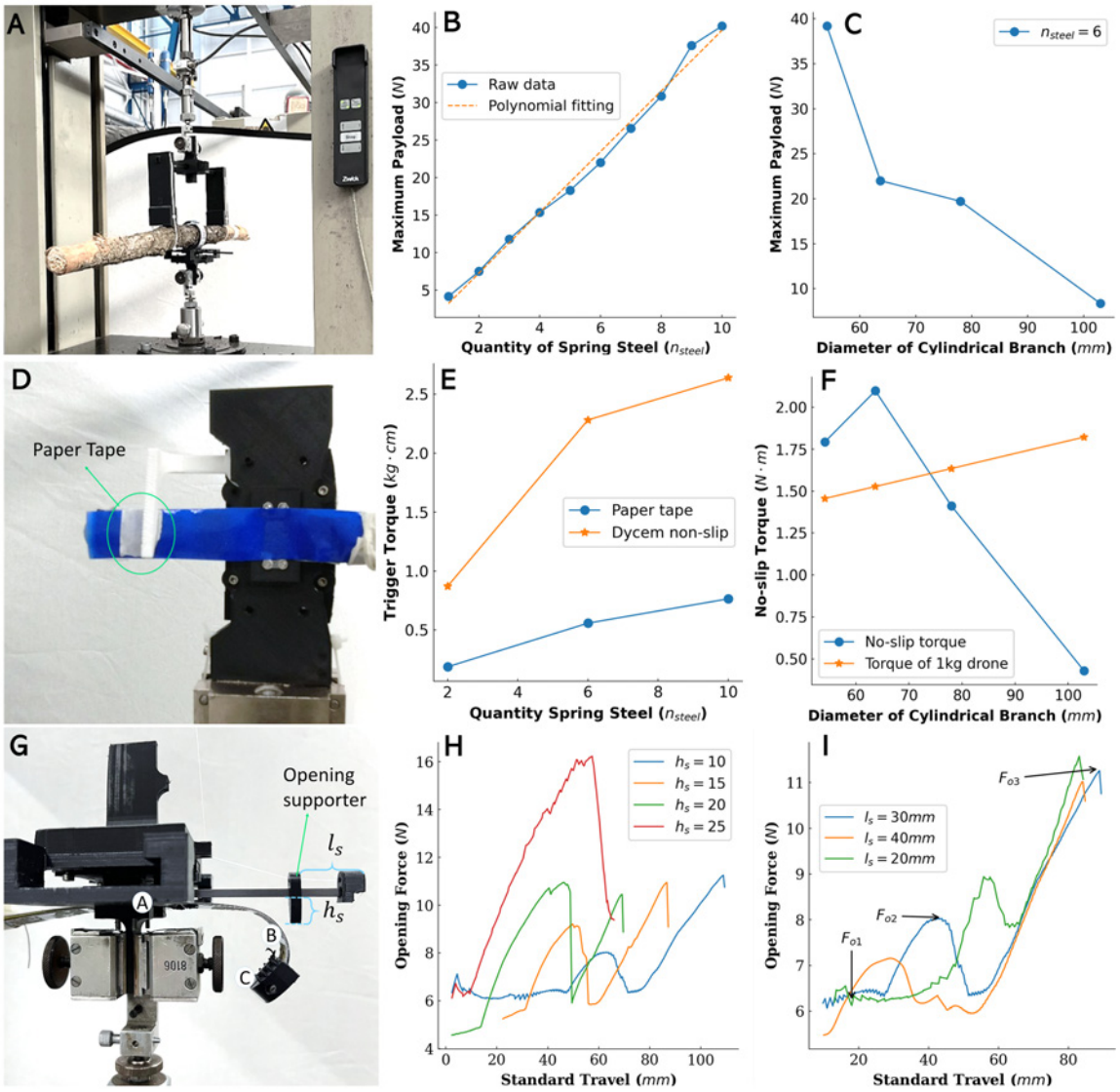

Fig. 5: Experimental results of ALBERO's active perching mechanism: (A) maximum payload experiments, (B) different numbers of steel layers with a regression linear function for $r_g = 0.2m$, (C) maximum load experiments for $n_{steel} = 6$ on different-sized branches, (D) trigger force experiments, (E) torque required to activate the trigger with different surface materials and n_{steel}, (F) torque required to prevent slipping of the gripper on different-sized branches at $\theta_g = 90^o$ and $n_{steel} = 6$, (G) opening force characterization experiments, (H) force required to open the finger at different h_s supporter positions for $n_{steel} = 6$, and (I) force required to open the finger at different l_s supporter positions for $n_{steel} = 6$.

0.95kg (Fig.1) and 0.148kg (Fig.7), respectively. The detailed parameters are provided in Table 1. The maximum payload capacity was tested using a branch with a 20 cm diameter.

TABLE I: Grippers' Parameters.

Name	Big Drone	Small Drone
Drone Weight (g)	950	148
Number of metal steel	6	2
360 servo	Feetech STS3032	MG90S
360 Torque (kg·cm) [weight (g)]	4.5 [20]	2.0 [14]
180 servo	Feetech STS3032	AGFRC servo
180 Torque (kg·cm) [weight (g)]	4.5 [20]	0.17 [1.5]
Gripper total weight (g)	142	35
Maximum payload (N)	22	10.7
Gripper payload-to-weight ratio	15.8	31.2

G. Agile Perching Indoor Experiments

Based on the results of the mechanical experiments, we carefully selected appropriate equipment to design the gripper. Furthermore, we validated the performance of the motion planner jointly with the gripper's via actual flight tests. Our flight platform utilized a 5-inch propeller drone, with a total weight of 0.95kg. The onboard computer was equipped with Nvidia NX software, while the flight controller used Pixracer, running PX4 firmware.

We conducted tests with branch inclinations of 0^o, 20^o, and 40^o, as illustrated in Fig.6A-C. To ensure a successful perching maneuver, we set the desired terminal norm velocity $v(T) = 0m/s$ to prevent the drone from bouncing off the branch. Other constraint parameters were configured as

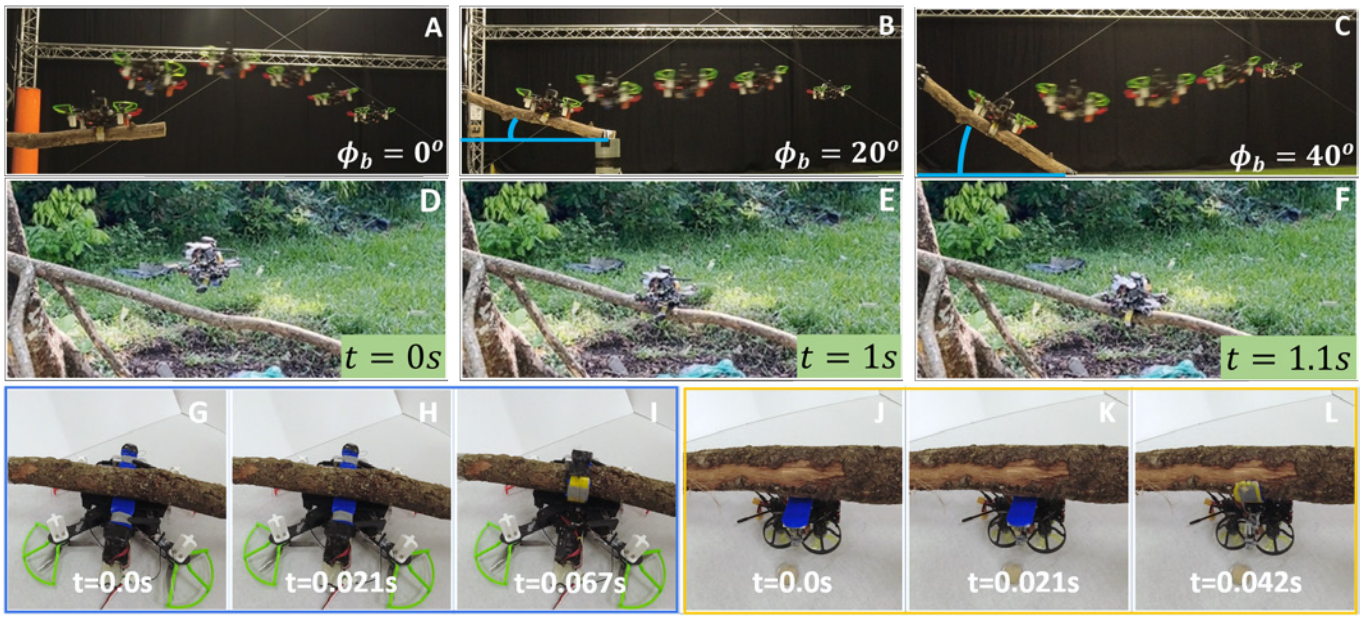

Fig. 6: Indoor agile perching (A-C), outdoor manual perching (D-F), big gripper closing (G-I) and small gripper closing (J-L).

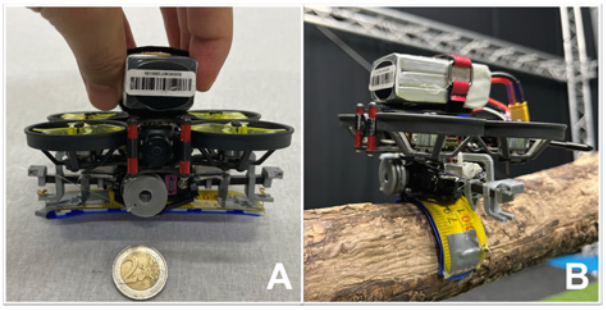

Fig. 7: (A) Miniaturised gripper mounted on a 148g micro drone, (B) manual perching.

follows: $v_{\max} = 2m/s$, $\omega_{\max} = 4rad/s$, and $\tau_{\max} = 8m/s^2$. Currently, this project does not utilize visual information. Instead, motion capture is employed to obtain drone and branches position and orientation. The experiments were conducted in TU Delft's Cyberzoo, where inclined tree branches were fixed onto a truss structure inside the flight arena. The drone took off from various positions and, utilizing the aforementioned planning approach, generated trajectories in real time. During the experiments, we observed that although ALBERO's gripper can complete the grasping within 0.067 seconds, this short duration is still impossible for the drone to maintain a stable inclined attitude mid-air. Therefore, in trajectory planning, a signal is sent to the gripper 0.05 seconds before the trajectory endpoint to ensure accurate grasping. Fig.8 illustrates the drone's state while perching on a 40° inclined branch. The maximum velocity is limited to 2 m/s, and the maximum angular velocity is limited to 4 rad/s. Fig. 8(C) indicates that the total acceleration of the drone upon contact with the branch is approximately 5 m/s^2, resulting in a force of around 5.5 N due to the drone's takeoff weight of 1.1 Kg. This force falls within the gripper's load-bearing capacity of 22N, thus allowing the drone to successfully perch on the tree branch.

H. Outdoor Perching Experiments

We also conducted outdoor tests focusing on perch experiments involving slightly inclined tree branches. These tests were carried out without the incorporation of stereoscopic visual information and in the absence of precise outdoor positioning data. To facilitate this, we uniquely positioned an FPV (First Person View) camera on the front underside of the drone. This camera placement enables us to determine the tree branch's relative position in relation to the drone. Once the drone makes contact with the branch, remote control inputs are used to activate the gripper's grasping action. By exclusively relying on visual feedback provided by the FPV camera, we executed perching maneuvers. The results demonstrated that the drone consistently managed to secure a hold of the tree branch and successfully take off again. Fig. 6D-F showcases three distinct moments from one of these experimental trials.

V. Conclusion

In this article, we introduce ALBERO: a framework that encompasses new hardware and software to realise agile dynamic perching manoeuvres of quadrotors on real tree branches. The novel active gripper design has four key attributes: ultra-fast grasping, high power-to-weight ratio, scalability, and exceptional energy efficiency. The remarkably swift grasping speed ensures the drone's effective perching on steeply inclined branches, as realistically found in the real world. Our mechatronic solution is complemented by a dedicated motion planner to achieve the dynamic constraints posed by agile perching maneuvers. The proposed planner demonstrates successful dynamic quadrotor perching on inclined branches via real flight experiments. Future work in this direction will look into incorporating accurate pose estimation outdoors by means of computer vision methods, for reliable perching manoeuvres in the real world.

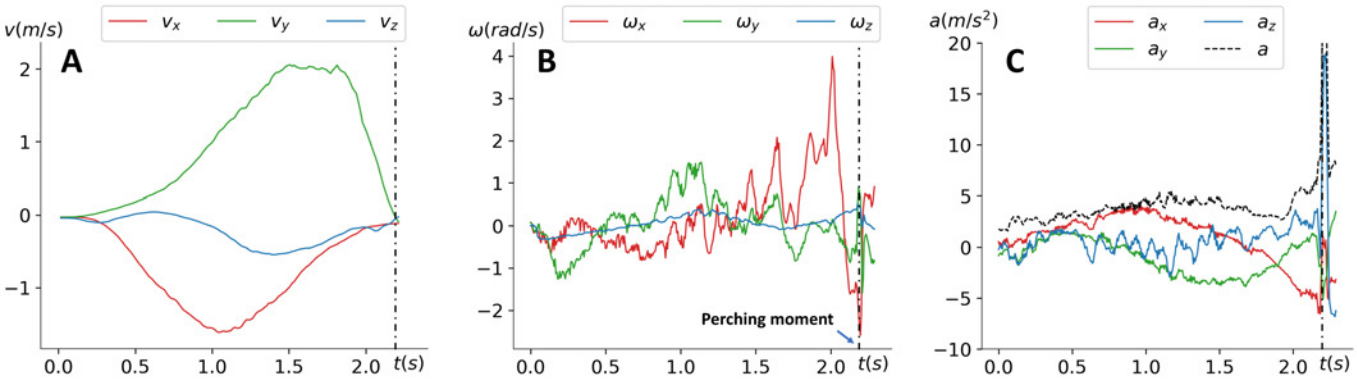

Fig. 8: Flight data of agile perching on 40^o angled branch: A) ground truth velocities are zero at hover state ($t = 0s$) and prior to the perched state ($t \approx 2.2s$), B) body rate, and C) accelerations of the drone measured onboard.

ACKNOWLEDGEMENTS

We thank Hang Yu for assisting with flight experiments.

REFERENCES

[1] J.-F. Bastin, Y. Finegold, C. Garcia, D. Mollicone, M. Rezende, D. Routh, C. M. Zohner, and T. W. Crowther, "The global tree restoration potential," *Science*, vol. 365, no. 6448, pp. 76–79, 2019.

[2] J. E. Watson, T. Evans, O. Venter, B. Williams, A. Tulloch, C. Stewart, I. Thompson, J. C. Ray, K. Murray, A. Salazar *et al.*, "The exceptional value of intact forest ecosystems," *Nature ecology & evolution*, vol. 2, no. 4, pp. 599–610, 2018.

[3] *XPRIZE Rainforest, https://rainforest.xprize.org/prizes/rainforest*.

[4] A. Nakamura, R. L. Kitching, M. Cao, T. J. Creedy, T. M. Fayle, M. Freiberg, C. Hewitt, T. Itioka, L. P. Koh, K. Ma *et al.*, "Forests and their canopies: achievements and horizons in canopy science," *Trends in ecology & evolution*, vol. 32, no. 6, pp. 438–451, 2017.

[5] L. F. Oliveira, A. P. Moreira, and M. F. Silva, "Advances in forest robotics: A state-of-the-art survey," *Robotics*, vol. 10, no. 2, p. 53, 2021.

[6] S. Hamaza, I. Georgilas, M. Fernandez, P. Sanchez, T. Richardson, G. Heredia, and A. Ollero, "Sensor installation and retrieval operations using an unmanned aerial manipulator," *IEEE Robotics and Automation Letters*, vol. 4, no. 3, pp. 2793–2800, 2019.

[7] S. Hamaza, H. Nguyen, and M. Kovac, "Sensor delivery in forests with aerial robots: A new paradigm for environmental monitoring," in *IEEE IROS Workshop on Perception, Planning and Mobility in Forestry Robotics*, 2020.

[8] C. Geckeler and S. Mintchev, "Bistable helical origami gripper for sensor placement on branches," *Advanced Intelligent Systems*, vol. 4, no. 10, p. 2200087, 2022.

[9] E. Aucone, S. Kirchgeorg, A. Valentini, L. Pellissier, K. Deiner, and S. Mintchev, "Drone-assisted collection of environmental dna from tree branches for biodiversity monitoring," *Science Robotics*, vol. 8, no. 74, p. eadd5762, 2023.

[10] M. A. Graule, P. Chirarattananon, S. B. Fuller, N. T. Jafferis, K. Y. Ma, M. Spenko, R. Kornbluh, and R. J. Wood, "Perching and takeoff of a robotic insect on overhangs using switchable electrostatic adhesion," *Science*, vol. 352, no. 6288, pp. 978–982, 2016.

[11] C. Ramos-Romero, N. Green, S. Roberts, C. Clark, and A. J. Torija, "Requirements for drone operations to minimise community noise impact," *International Journal of environmental research and public health*, vol. 19, no. 15, p. 9299, 2022.

[12] D. King and O. L. Loucks, "The theory of tree bole and branch form," *Radiation and environmental biophysics*, vol. 15, pp. 141–165, 1978.

[13] A. Bressan and Q. Sun, "On the optimal shape of tree roots and branches," *Mathematical Models and Methods in Applied Sciences*, vol. 28, no. 14, pp. 2763–2801, 2018.

[14] S. Tsugawa, K. Teratsuji, F. Okura, K. Noshita, M. Tateno, J. Zhang, and T. Demura, "Exploring the mechanical and morphological rationality of tree branch structure based on 3d point cloud analysis and the finite element method," *Scientific reports*, vol. 12, no. 1, p. 4054, 2022.

[15] W. Chi, K. Low, K. H. Hoon, and J. Tang, "An optimized perching mechanism for autonomous perching with a quadrotor," in *2014 IEEE international conference on robotics and automation (ICRA)*. IEEE, 2014, pp. 3109–3115.

[16] F. Ruiz, B. C. Arrue, and A. Ollero, "Sophie: Soft and flexible aerial vehicle for physical interaction with the environment," *IEEE Robotics and Automation Letters*, vol. 7, no. 4, pp. 11 086–11 093, 2022.

[17] P. Zheng, F. Xiao, P. H. Nguyen, A. Farinha, and M. Kovac, "Metamorphic aerial robot capable of mid-air shape morphing for rapid perching," *Scientific Reports*, vol. 13, no. 1, p. 1297, 2023.

[18] W. R. Roderick, M. R. Cutkosky, and D. Lentink, "Bird-inspired dynamic grasping and perching in arboreal environments," *Science Robotics*, vol. 6, no. 61, p. eabj7562, 2021.

[19] J. Thomas, G. Loianno, K. Daniilidis, and V. Kumar, "Visual servoing of quadrotors for perching by hanging from cylindrical objects," *IEEE robotics and automation letters*, vol. 1, no. 1, pp. 57–64, 2015.

[20] K. M. Popek, M. S. Johannes, K. C. Wolfe, R. A. Hegeman, J. M. Hatch, J. L. Moore, K. D. Katyal, B. Y. Yeh, and R. J. Bamberger, "Autonomous grasping robotic aerial system for perching (agrasp)," in *2018 IEEE/RSJ international conference on intelligent robots and systems (IROS)*. IEEE, 2018, pp. 1–9.

[21] K. Hang, X. Lyu, H. Song, J. A. Stork, A. M. Dollar, D. Kragic, and F. Zhang, "Perching and resting—a paradigm for uav maneuvering with modularized landing gears," *Science Robotics*, vol. 4, no. 28, p. eaau6637, 2019.

[22] R. Zufferey, J. Tormo-Barbero, D. Feliu-Talegón, S. R. Nekoo, J. Á. Acosta, and A. Ollero, "How ornithopters can perch autonomously on a branch," *Nature Communications*, vol. 13, no. 1, p. 7713, 2022.

[23] J. Ji, T. Yang, C. Xu, and F. Gao, "Real-time trajectory planning for aerial perching," in *2022 IEEE/RSJ International Conference on Intelligent Robots and Systems (IROS)*. IEEE, 2022, pp. 10 516–10 522.

[24] J. Mao, S. Nogar, C. M. Kroninger, and G. Loianno, "Robust active visual perching with quadrotors on inclined surfaces," *IEEE Transactions on Robotics*, 2023.

[25] H. Jiang, M. T. Pope, E. W. Hawkes, D. L. Christensen, M. A. Estrada, A. Parlier, R. Tran, and M. R. Cutkosky, "Modeling the dynamics of perching with opposed-grip mechanisms," in *2014 IEEE international conference on robotics and automation (ICRA)*. IEEE, 2014, pp. 3102–3108.

[26] J. Thomas, M. Pope, G. Loianno, E. W. Hawkes, M. A. Estrada, H. Jiang, M. R. Cutkosky, and V. Kumar, "Aggressive flight with quadrotors for perching on inclined surfaces," *Journal of Mechanisms and Robotics*, vol. 8, no. 5, p. 051007, 2016.

[27] Z. Wang, X. Zhou, C. Xu, and F. Gao, "Geometrically constrained trajectory optimization for multicopters," *IEEE Transactions on Robotics*, vol. 38, no. 5, pp. 3259–3278, 2022.

[28] P. H. Nguyen, K. Patnaik, S. Mishra, P. Polygerinos, and W. Zhang, "A soft-bodied aerial robot for collision resilience and contact-reactive perching," *Soft Robotics*, 2023.

[29] J. L. Paneque, J. R. Martínez-de Dios, A. Ollero, D. Hanover, S. Sun, A. Romero, and D. Scaramuzza, "Perception-aware perching on powerlines with multirotors," *IEEE Robotics and Automation Letters*, vol. 7, no. 2, pp. 3077–3084, 2022.

[30] M. W. Mueller, M. Hehn, and R. D'Andrea, "A computationally efficient motion primitive for quadrocopter trajectory generation," *IEEE Transactions on Robotics*, vol. 31, no. 6, pp. 1294–1310, 2015.